

Supplement of Atmos. Meas. Tech., 10, 4833–4844, 2017
<https://doi.org/10.5194/amt-10-4833-2017-supplement>
© Author(s) 2017. This work is distributed under
the Creative Commons Attribution 4.0 License.



Supplement of

A new non-resonant laser-induced fluorescence instrument for the air-borne in situ measurement of formaldehyde

Jason M. St. Clair et al.

Correspondence to: Jason M. St. Clair (jason.m.stclair@nasa.gov)

The copyright of individual parts of the supplement might differ from the CC BY 4.0 License.

Table S1: AJAX flight information with COFFEE in payload, through March 2017.

Flight date	AJAX flight number	Flight objective
12/15/2015	F178	Test flight; San Joaquin Valley
01/08/2016	F179	Aliso Canyon methane leak
01/12/2016	F180	Railroad Valley for CH ₄ /CO ₂ satellite validation
03/17/2016	F182	Boundary layer sampling around Sacramento
03/23/2016	F183	Aliso Canyon after methane leak capped
03/30/2016	F184	Level boundary layer legs in the San Joaquin Valley
04/19/2016	F185	San Joaquin Valley (onshore) and offshore vertical profiles
04/26/2016	F186	Vertical profiles at Visalia, Panoche, and Bodega Bay
05/04/2016	F187	Two onshore and one offshore vertical profiles
05/12/2016	F188	Offshore vertical profiles under OCO-2 satellite
06/15/2016	F191	Vertical profiles offshore (Bodega Bay) and onshore (Visalia); fire sampling
06/21/2016	F192	Vertical profiles at Point Sur, Chews Ridge, Panoche, Visalia
07/01/2016	F193	Railroad Valley for CH ₄ /CO ₂ satellite validation
07/21/2016	F195	Vertical profiles offshore near Bodega Bay and over land near Visalia
07/28/2016	F196	Soberanes Fire
08/09/2016	F197	Soberanes Fire
08/12/2016	F198	Soberanes Fire
08/24/2016	F199	Soberanes and Cedar Fires
09/14/2016	F200	Soberanes Fire
09/21/2016	F201	Vertical profiles and level legs in the San Francisco Bay Area: offshore, San Martin, Patterson Pass, Bethel Island
11/02/2016	F202	Vertical profiles and level legs in the San Francisco Bay Area: Bodega Bay, Pittsburg/Delta, East San Jose
11/03/2016	F203	Vertical profiles and level legs in the San Francisco Bay Area: offshore, Bethel Island, Livermore, East San Jose
12/02/2016	F204	Chews Ridge and MMS calibration maneuvers
02/23/2017	F207	Vertical profiles and level legs in the San Francisco Bay Area: Bodega Bay, Bethel Island, San Martin
03/01/2017	F208	Vertical profiles and level legs in the San Francisco Bay Area: Bodega Bay, Bethel Island, San Martin, Livermore
03/09/2017	F209	Boundary layer legs along Walker and Tehachapi Passes, Antelope Valley
03/23/2017	F210	Boundary layer legs along San Pablo Bay, Sacramento River Delta, McDonald Island

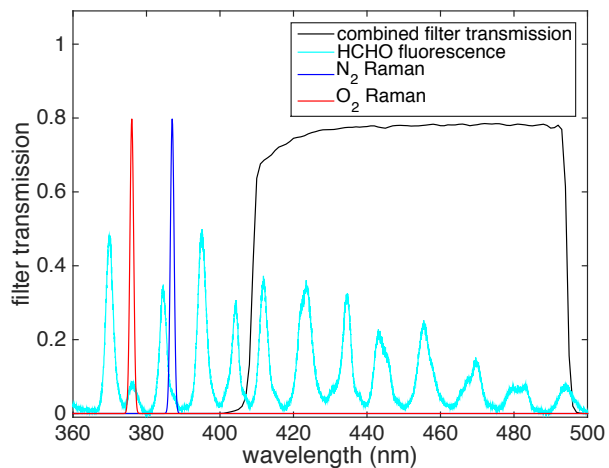


Figure S1: The optical filter transmission spectrum is shown for detection axis 1 (450 nm band pass filter). The HCHO fluorescence and the N_2 and O_2 Raman spectra are included for reference, all with arbitrary units.

5

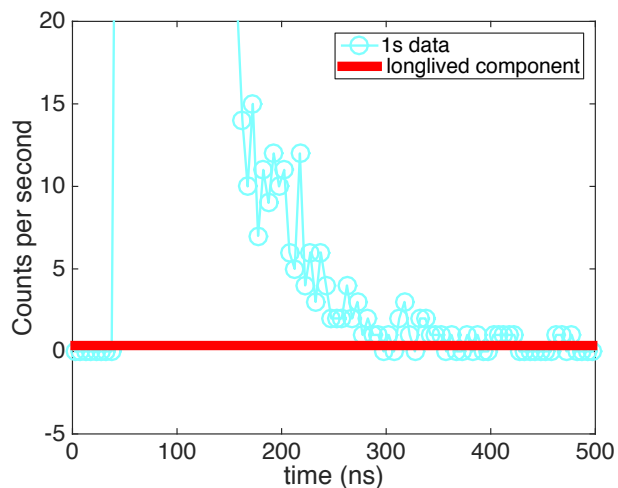
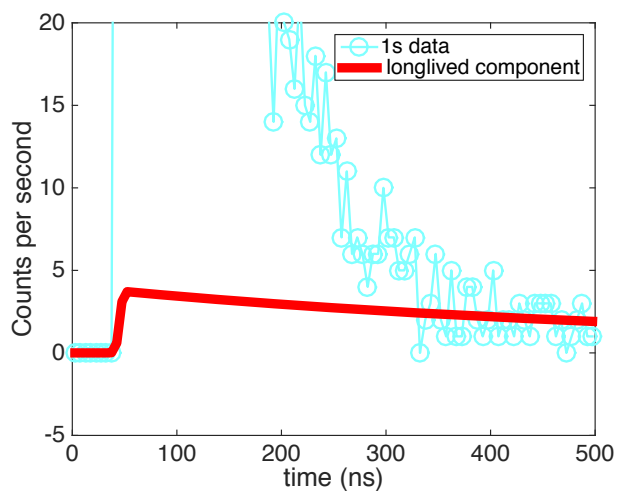
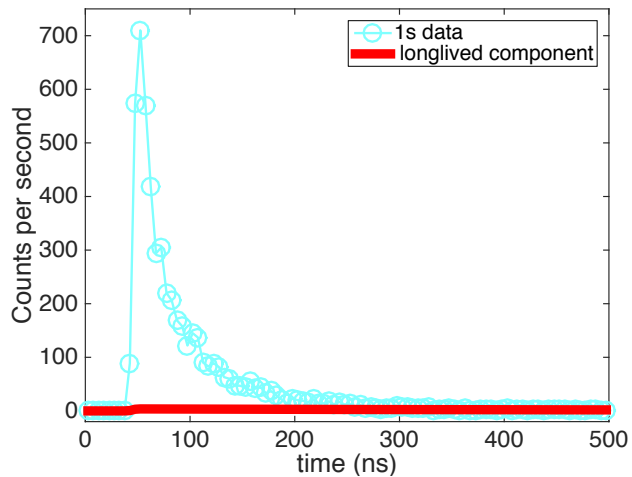


Figure S2: Detection axis 2 time profile (cyan circles) and corresponding long-lived component (red line) that is subtracted before performing exemplar fits. The time profile is the same 1 s of data shown in Figure 5.

10

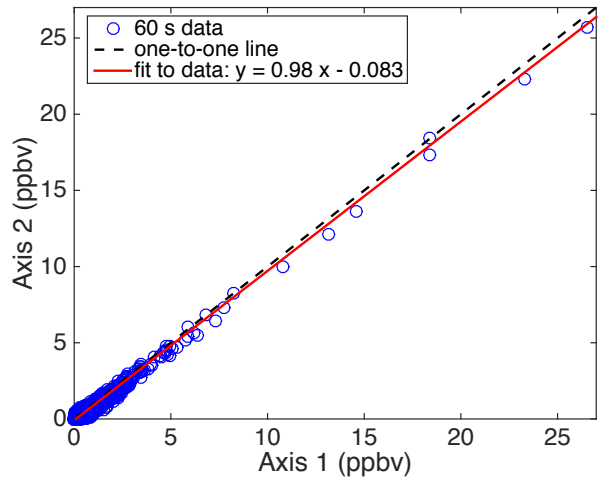


5

Figure S3: Top Panel: Detection axis 1 time profile (cyan circles) and corresponding long-lived component (red line) that is subtracted before performing exemplar fits. The time profile is the same 1 s time period as shown in Fig. 5 and Fig. S2 for detection axis 2. Bottom Panel: Same data as the Top Panel, with different y-axis range.

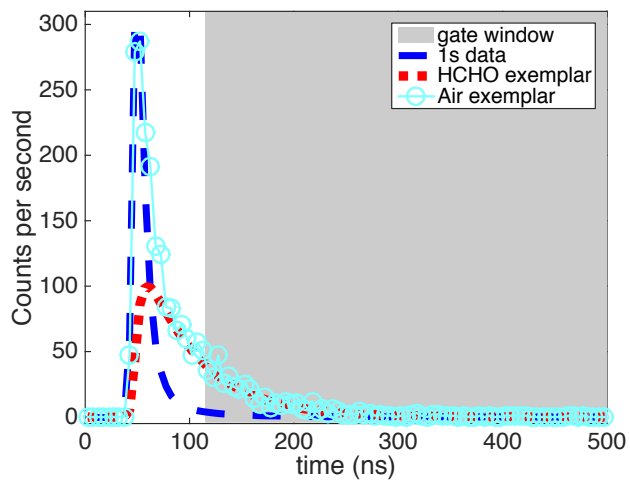
10

15



5

Figure S4: Comparison of 60 s averaged data from axis 1 and axis 2.



10 Figure S5: Time profile from Fig. 5 with shaded region indicating the window for gated counts.

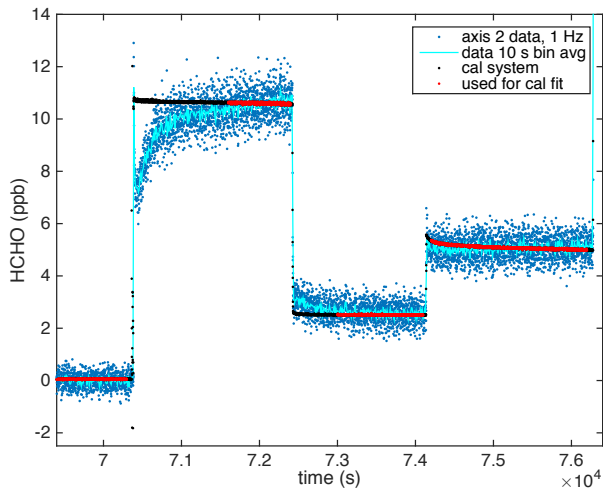


Figure S6: Calibration data from the multi-band pass filter detection axis (axis 2), using the exemplar fitting technique to process the data. Note that the slow time response is due to the calibration system and not the instrument—instrument time response is addressed in Sect. 4.4.

5

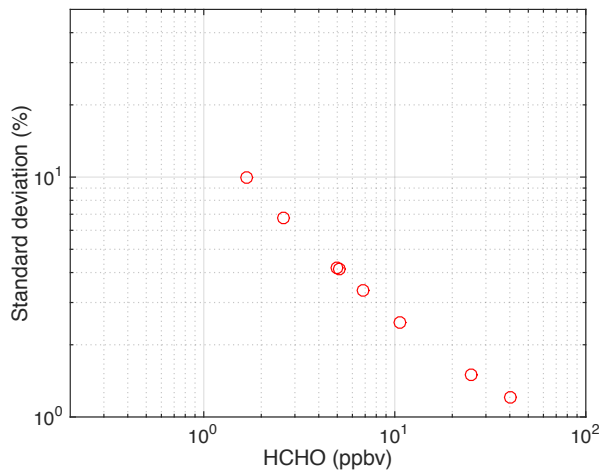


Figure S7: The standard deviation for 1 s data normalized by the mean HCHO is shown as a function of HCHO to demonstrate the precision of the HCHO measurement.